Int. J. Electrochem. Sci., 8 **(2013)** 6068 - 6076

International Journal of
ELECTROCHEMICAL
SCIENCE
www.electrochemsci.org

Palladium Decorated Nickel Nanoparticles Supported on Carbon for Formic Acid Oxidation

Ronfang Wang[1,*], *Hui Wang*[1], *Hanqing Feng*[2], *Shan Ji*[3,*]

[1] Key Laboratory of Eco-Environment-Related Polymer Materials, Ministry of Education of China, Key Laboratory of Gansu Polymer Materials, College of Chemistry and Chemical Engineering, Northwest Normal University, Lanzhou 730070, China
[2]College of Life Science, Northwest Normal University, Lanzhou 730070, China
[3]South African Institute for Advanced Materials Chemistry, University of the Western Cape, South Africa
[*]E-mail: wangrf@nwnu.edu.cn; sji@uwc.ac.za

Received: 23 August 2012 / *Accepted:* 8 April 2013 / *Published:* 1 May 2013

Carbon-supported palladium decorated nickel nanoparticles (denoted as Pd@Ni/C) with intimate contact of Pd and Ni was prepared by a two-step method. A series of characterizations were performed using transmission electron microscopy (TEM), X-ray diffraction (XRD) and electrochemical techniques. The results of XRD and TEM proved the Pd decorated Ni structure. Electrochemical results showed that Pd@Ni/C had a higher mass activity and stability to formic acid oxidation reaction than conventional Pd/C, which could be attributed to the modified electronic structure of Pd decorated nickel nanoparticles.

Keywords: Decorated; Electrocatalysts; Fuel Cells; Formic Acid Oxidation; Electrooxidation

1. INTRODUCTION

Direct formic acid fuel cells (DFAFCs) are attractive energy conversion devices for powering portable electronics by converting the chemical energy of formic acid directly into electricity [1-4]. Fabrication of active electrocatalysts with low noble metal loading for anode is essential for the DFAFCs development [5]. Therefore, many efforts have focused on the development of techniques and new materials to achieve high catalytic activity and high utilization of noble metal. Due to the lower cost and higher catalysis toward formic acid electro-oxidation as compared to those of Pt/C, high performance Pd/C is the focus of recent investigations [6-10]. However, the electrocatalytic activity and stability of pure Pd are still not satisfied for the requirement of its commercialization. The activity

of electrocatalysts strongly depends on the electronic, structural, and geometric properties of metallic materials. Therefore, a lot of effort has been made by designing special nanostructures or alloying with a second element to achieve the high performance and stability of Pd-based catalysts [11-13].

To increase the formic acid oxidation activity and further reduce noble-metal loading, bimetallic catalysts of palladium alloyed with a less expensive metal M (M = Fe, Co, Ni, and Cu etc.) are often used [14-18]. Among different bimetallic catalysts, PdNi has attracted a lot of attention owing to its strong formic acid oxidation enhancement [17, 19-23]. The improved catalytic activity is explained by bifunctional mechanism and electronic effect [20-22]. In the bifunctional mechanism, the palladium sites are responsible for formic acid oxidation to form adsorbed carbon monoxide (CO_{ads}), which poisons the catalyst surface for further fuel oxidation; the nickel sites provide adsorbed hydroxyl groups (OH_{ads}), which is favor the oxidant for the removal of CO_{ads} [20, 23]. At a same time, nickel may also hinder the adsorption of the HCOO during formic acid electro-oxidation [17]. In the electronic effect, the presence of nickel changes the electronic structure of palladium in a way that it lowers the CO adsorption energy [23]. These two mechanisms often operate simultaneously and are frequently used to explain the activity enhancement of other Pd/M alloys.

Core-shell structure at an atomic scale is an efficient way to improve the utilization efficiency of active materials and enhance the electrocatalytic activities towards formic acid and methanol oxidation [24-27]. Recently, a two-step reduction method to prepare carbon supported Pt-based and Pd-based core-shell structrue electrocatalysts has been developed by our group. These Pd-based electrocatalysts have demonstrated higher mass activity than the conventional Pt/C and Pd/C catalysts in fuel cell systems [28-30]. We also developed Pt decorated Ni nanoparticles as catalysts for methanol oxidation and oxygen reduction, and found that Pt decoration is an effective method to improve the utilization of noble metals [31, 32]. Based on these previous studies, it will be meaningful to explore the carbon-supported Pd decorated Ni catalyst prepared by chemical reduction for formic acid oxidation.

In this study, a modified two-step method was developed to prepare carbon supported palladium decorate nickel nanoparticles (Pt@Ni/C), which was evaluated by formic acid oxidation reaction. The morphologic properties and electrochemical behaviors of synthesized catalysts were investigated.

2. EXPERIMENTAL

2.1 Preparation of Pd@Ni/C catalyst

Pd@Ni catalyst was prepared by a two-step method. In a typical process, carbon supported Ni nanoparticles were prepared by as follows: nickel (II) chloride hexahydrate ($NiCl_2 \cdot 6H_2O$) (303 mg) and sodium were dissolved in solution containing 25 mL water and 25 mL ethanol. Then 750 mg of sodium citrate was introduced into above solution. The pH of the system was adjusted by the addition of 3 g of KOH with vigorous stirring for 0.5 h. The carbon black Vulcan® XC-72 (300 mg, pretreated by 2 mol L^{-1} of HNO_3 and 3% H_2O_2) was added to the mixture under stirring conditions. Subsequently,

15 mL of hydrazine hydrate was added. The mixture was then transferred to a Teflon lined autoclave and the temperature was kept to 120 ºC for 4 h. The product was collected by filtration, washed with deionized water 5~8 times and dried in vacuum oven at 60 °C for 12 h.

Subsequently, 41.7 mg of $PdCl_2$ was transferred into a 100 mL beaker. Two drops of concentrated HCl acid was added to beaker, and then the mixture was treated in ultrasonic bath for several minutes. After that, 30 mL of ethylene glycol (EG) were introduced into the $PdCl_2$ mixture. Its pH was adjusted to 10 by adding 5% KOH/EG solution. The obtained Ni/C powder was transferred to the flask and sonicated for 30 mins. Subsequently, the mixture was heated at 160 ^oC for 6 h. The product was collected by filtration, rinsed with deionized water for 8~10 times and dried overnight in a vacuum oven.

2.2 Characterization

The catalysts were characterized by recording their XRD patterns on a Shimadzu XD-3A (Japan), using filtered Cu-Kα radiation. All X-ray diffraction patterns were analyzed using Jade 7.5 of Material Data, Inc. (MDI): peak profiles of individual reflections were obtained by a nonlinear least-square fit of the Cu Kα corrected data. Transmission electron microscopy (TEM) measurements were carried out on a JEM-2010 Electron Microscope (Japan) with the acceleration voltage of 200 kV.

The electrochemical measurements of catalysts are performed using an Autolab electrochemical work station (PGSTAT128N). A common three-electrode electrochemical cell was used for the measurements. The counter and reference electrode were a platinum wire and an Ag/AgCl (3 M KCl) electrode, respectively. The working electrode was a glassy carbon disk (5 mm in diameter). The thin-film electrode was prepared as follows: 5 mg of catalyst was dispersed ultrasonically in 1 mL Nafion/ethanol (0.25% Nafion) for 15 min. 8 μL of the dispersion was transferred onto the glassy carbon disk using a pipette, and then dried in the air. The catalysts were characterized by cyclic voltammetry (CV) and chronoamperometry (CA) tests at room-temperature. Before each measurement, the solution is purged with high purity N_2 gas for at least 30 min to ensure O_2 free measurements.

3. RESULTS AND DISCUSSION

The carbon-supported Pd@Ni/C was synthesized via a sequential reduction process. First, the core was synthesized by a modified organic colloid method in an ethylene glycol solution; Second, the $PdCl_4^{2-}$ was mainly reduced by EG, and simultaneously some of the atoms in the outer layer of the Ni core were also sacrificed to reduce $PdCl_4^{2-}$. Under such conditions, Pd shell can be expected to form on the surface of Ni cores. Pd atoms can deposit on Ni nanoparticles, which could be attributed to: the palladium and nickel are metallic crystal with face centered cubic (fcc) structure, and the interaction between the Pd and Ni meta is stronger than that between Pd and carbon support, which is in favor of the Pd growth on the Ni nanoparticle surface.

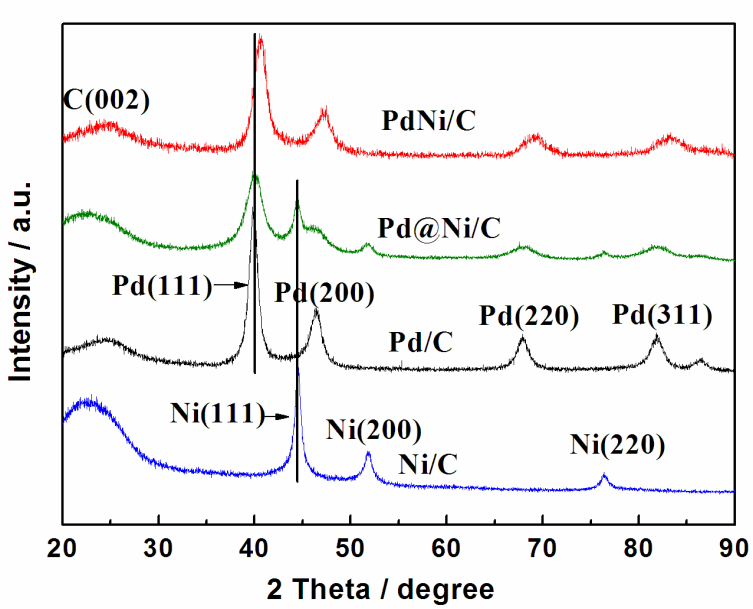

Figure 1. XRD patterns of Pd/C, PdNi/C, Ni/C, and Pd@Ni/C catalysts.

Figure 1 shows the XRD patterns of Pd@Ni/C, Pd/C, and Ni/C nanoparticles. For comparison, carbon-supported PdNi alloy (PdNi/C, Pd/Ni=2:1 in atomic ratio) catalyst prepared by the polyol method is also shown in this figure. The first peak located at about 24.8 in all the XRD patterns is associated with the carbon support. For the Ni/C, all of the peaks match well with Bragg reflections of the standard fcc structure (ICDD file no: 04-0850, space group: Fm3m (225)), the three peaks at 44.5^o, 51.8^o and 76.3^o can be assigned to their characteristic (111), (200) and (220) indices. The lattice parameter of the Ni/C nanoparticles was found to be 0.352 nm. This is in agreement with the lattice parameter for bulk Ni. No characteristic peaks due to the impurities of nickel oxides were detected, which indicates that the Ni in Ni/C catalyst prepared by the this method is pure nickel.

For the Pd/C and PdNi/C alloy, the five peaks were located at 2θ values of ca. 40^o, 47^o, 68^o, 83^o, and 86^o attributed to the characteristic (111), (200), (220), (311), and (222) planes of palladium crystalline, respectively. The XRD results indicate that the two catalysts possess face-centered cubic (fcc) crystalline structure. For the PdNi/C, only were the peaks corresponding to (111), (200), and (220) characteristic planes of Pd clearly observed. No diffraction peaks of either pure Ni or Ni-rich fcc phase were detected, indicating that Ni might enter into the Pd lattice forming PdNi alloy. It was also found that the diffraction peaks of PdNi/C shifted to high-angle values, suggesting that the lattice parameters of PdNi/C were decreased by addition of Ni.

In the XRD pattern of Pd@Ni/C catalyst, there are well separated diffraction peaks strongly suggest that there are different phases existed in Pd@Ni/C. Diffraction peaks at 44.5^o, 51.8^o and 76.3^o belong to metallic Ni, i.e. the Ni cores. No diffraction peaks were detected for Ni oxides species in XRD pattern. On the other hand, diffraction peaks around 40^o, 47^o, 68^o, 83^o, and 86^o, which are similar to the XRD pattern of Pd/C, are assigned to the Pd-shell. Compared to Pd/C and Ni/C, the diffraction peaks of shell and core for Pd@Ni/C samples are not shifted to higher angles or lower angles, indicating that no alloy phase was formed.

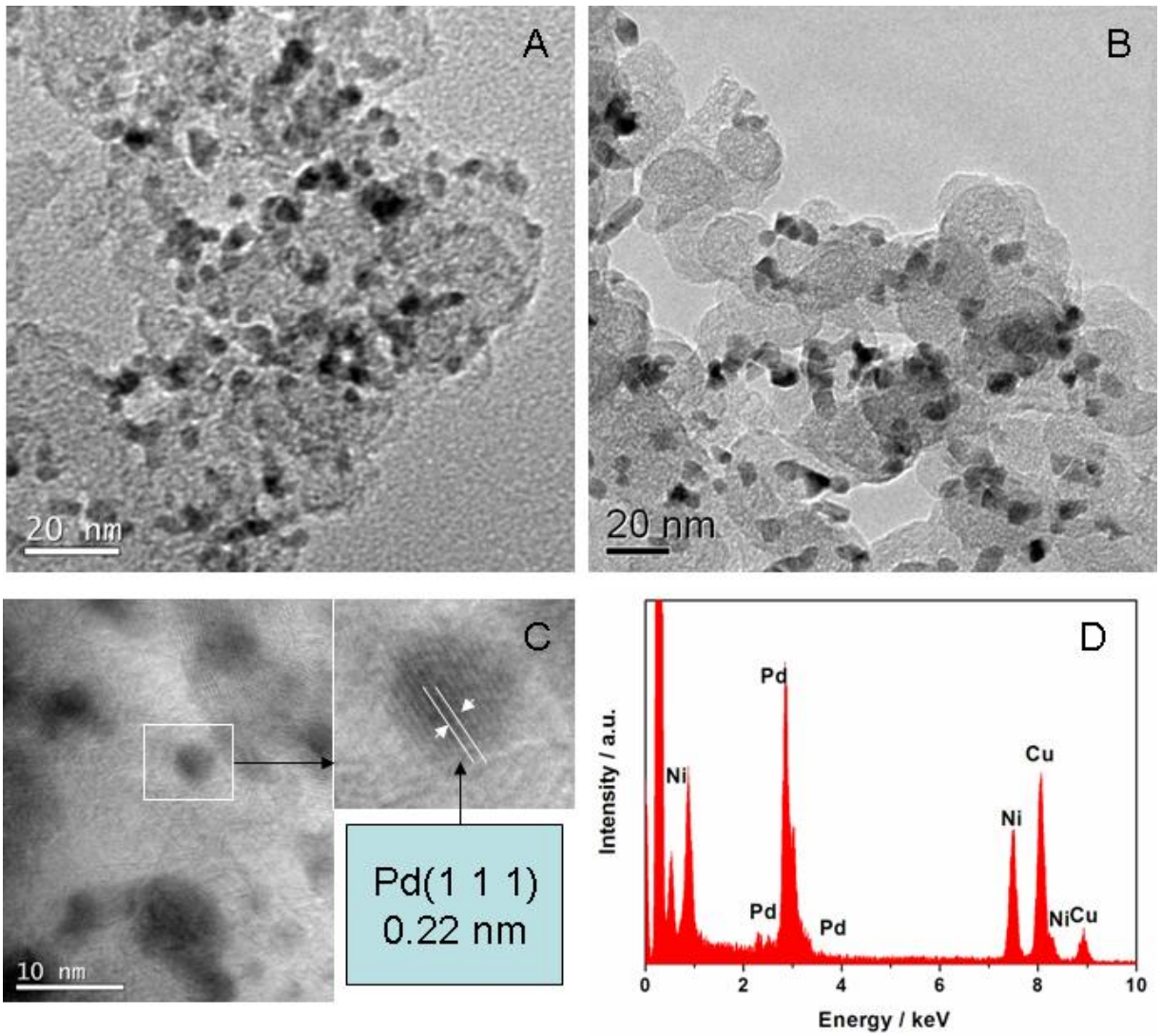

Figure 2. TEM images of Pd@Ni/C (A) and PdNi/C (B) catalysts; HRTEM of Pd@Ni/C (C); (D) EDX pattern of Pd@Ni/C catalysts.

Figure 2 (A) shows TEM image of Pd@Ni/C catalyst. For comparison, carbon-supported PtNi alloy catalyst is also shown in figure 2 (B). It is noted that the Pd@Ni and PtNi alloy nanoparticles are highly dispersed on the carbon support with narrow size distribution. The uniform nanoparticles dispersion of Pd@Ni/C catalyst may result from the precursor Ni nanoparticles distribution on carbon black in the process of the first step of Ni/C preparation. The average particle size of Pd@Ni/C catalyst is approximately 6–7 nm (obtained by counting one hundred particles), which is smaller than that of PdNi alloy (8-9 nm).

A high resolution transmission electron microscopy of a series of single Pd@Ni nanoparticle shows that each nanoparticle has a polycrystalline structure (Figure 2C). The measured distance between the two nearest atom rows for Pd@Ni/C is 0.22 nm, i.e., which is close to the (111) interplane distance of pure Pd, which further suggest Pd atoms are dispersed on the outer layer of Ni particles and not alloyed with Ni nanoparticles. The EDS result shows that Pd@Ni/C atomic ratio of Pt/Ni is about 1:2 (as shown in Figure 2D).

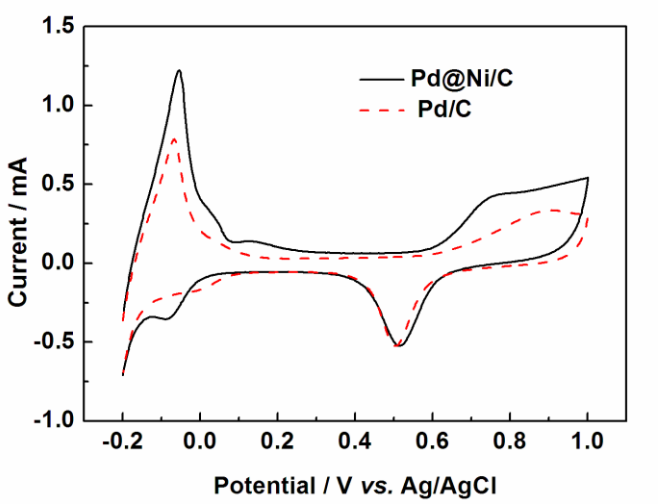

Figure 3. Cyclic voltammograms of Pd@Ni/C and Pd/C catalysts in 0.5 mol L^{-1} H_2SO_4 solution at 50 mV s^{-1} at room temperature

Another evidence for the Pd decorated Ni comes from cyclic voltammetry (CV) as it can be regarded as a surface sensitive technique that only detects the electrochemical properties of surface atoms rather than bulk atoms [31]. Figure 3 shows the CV of Pd/C and Pd@Ni/C catalysts in 0.5 M H_2SO_4. The shape of the profile is similar to the literature [23]. The multiple peaks between −0.2 V and 0.1 V vs. Ag/AgCl are attributed to the hydrogen absorption/desorption (H_{ab}) process. The smaller pair of peaks at the more positive potentials is thought to be an indication of real surface area of catalysts, and is missing or merged into the broad H_{ab} peaks sometimes.

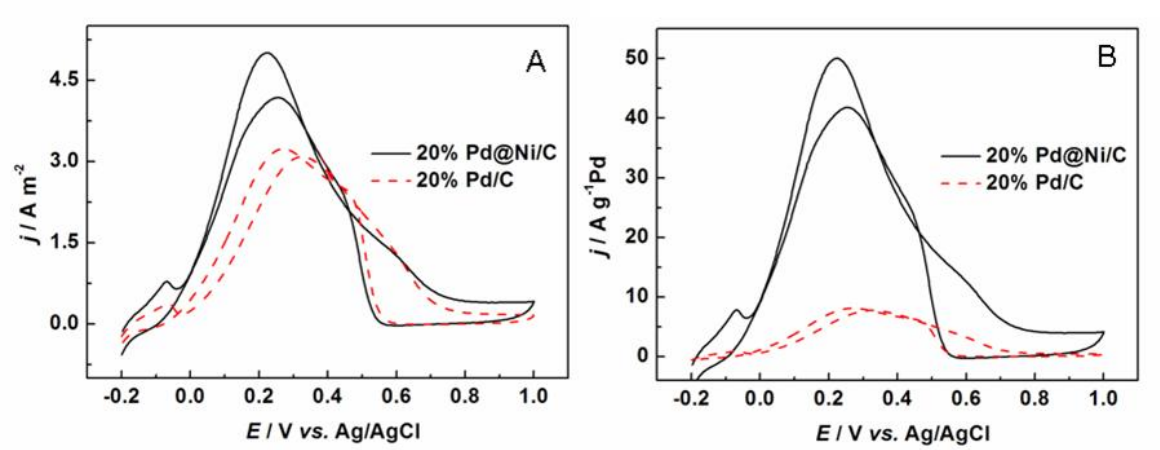

Figure 4. Cyclic voltammograms of formic acid electrooxidation on Pd@Ni/C and Pd/C in 0.5 mol L^{-1} HCOOH + 0.5 mol L^{-1} H_2SO_4 solution at 50 mV s^{-1} at room temperature. (A) Surface specific current and (B) mass specific current.

The double layer region between 0.1 V and 0.6 V vs. Ag/AgCl is mainly contributed by the carbon support. The observed difference in current of Pd oxidation after 0.6 V can be ascribed to the

difference of surface area. The electrochemical surface areas (EASA) of each catalyst was calculated from the density of charge associated with the reduction of a full monolayer of Pd oxides [6]. The EASA value are 64.5 $m^2\ g^{-1}_{metals}$ for Pd@Ni/C and 57.7 $m^2\ g^{-1}_{metals}$ for Pd/C. Based on the noble-metal mass, the ECSAs of Pd@Ni/C are 193.5 $m^2\ g^{-1}_{Pd}$, which is 3.35 times larger than that of Pd/C catalyst. The high ECSA is favorable to electrochemical reaction toward methanol oxidation. Figure 4 shows cyclic voltammograms of formic acid electrooxidation on the as-prepared catalysts in a solution of 0.5 M H_2SO_4 and 0.5 M HCOOH. The catalytic activity was evaluated by surface specific current (normalized to EASA, shown in Fig. 4A) and mass specific current (normalized to the mass of Pd, shown in Fig. 4B). A large current peak at potential range from 0-0.6 V was observed which is assigned to the reaction of formic acid oxidation via the direct pathway [33]. Apparently, the formic acid oxidation on the Pd and Pd@Ni catalysts is mainly through the direct pathway. The direct oxidation peak in the forward scan is usually used to evaluate the electrocatalytic activity of the catalysts. As observed, the surface specific current of the two catalysts for formic acid electroxidation Pd@Ni/C catalyst is about 1.5 times as high as that of Pd/C, which indicates the activity of catalysts is increased by the form of core-shell structure. In order to evaluate the mass activity of the catalysts, the current is normalized to the real mass for two catalysts. As observed, the mass current of the Pd@Ni/C for formic acid electroxidation is about 5.6 times higher than that of Pd/C.

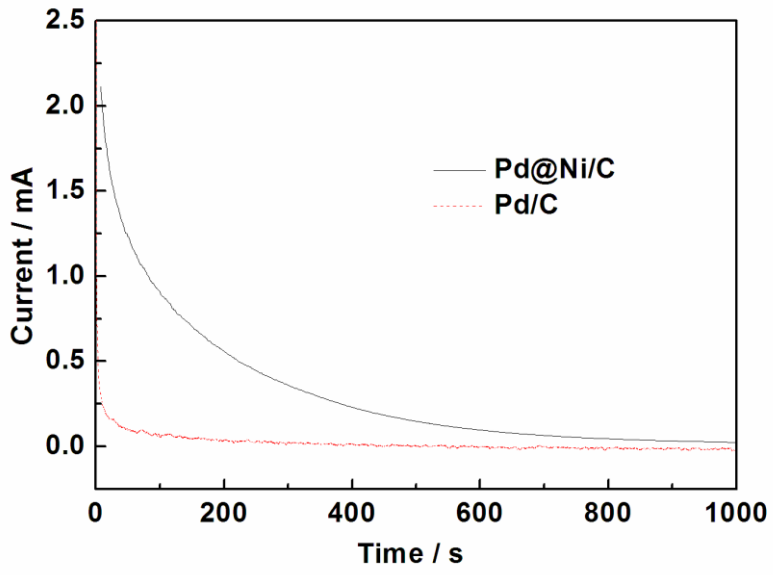

Figure 5. Chronoamperometric curves of Pd@Ni/C and Pd/C in 0.5 mol L^{-1} HCOOH + 0.5 mol L^{-1} H_2SO_4 solution at 0.1 V vs Ag/AgCl at room temperature

The stability of the electrocatalysts is extremely important for their real applications in DFAFCs. The long-term activity and durability of the Pd-based catalysts were further assessed by chronoamperometry, in which the potential was fixed at 0.1 V vs. Ag/AgCl, a typical working potential for formic acid oxidation in DFAFCs (Figure 5). As shown, the Pd@Ni/C catalyst has better catalytic activity and stability for formic acid electrooxidation. By combining cyclic voltammetry and

chronoamperometric results, it is concluded that the Pd@Ni/C catalyst has higher catalytic performance for formic acid electrooxidation than Pd/C, which demonstrates that the addition of an appropriate amount of Ni and core-shell structure can significantly improve the catalytic performance of Pd-based catalysts. The enhancement can be ascribed to the largely increased EASA and high dispersion combining with the electronic modification effect of nickel.

4. CONCLUSIONS

In summary, this study demonstrated a very general strategy to prepare carbon supported core-shell structure Pd@Ni/C catalysts with intimate contact of Pd and Ni. The structure has been proven by various techniques including XRD, TEM and electrochemical techniques. The electrocatalytic activity was evaluated by formic acid oxidation. The results show that core-shell catalyst with thin shell of Pd on Ni has a higher catalytic activity than Pd/C catalysts, which results in improved noble-metal utilization. The work further proves that catalytic activity of Pd catalyst towards formic acid oxidation can indeed be improved through controlling not only Pd nanoparticle size and shape but also its junction and interaction of non-noble metal nanoparticles. This structure has obvious advantages in terms of catalytic properties, simple processing, and saving noble metals, which is an efficient way to improve the catalytic activity for catalysts of DFAFCs.

ACKNOWLEDGMENTS
We greatly appreciate the National Natural Science Foundation of China (21163018), the National Science Foundation for Post-doctoral Scientists of China (20110490847), Guangdong Key Lab for Fuel Cell Technology and the South African NRF (SFP20110918000027143) for financially supporting this work.

References

1. C. Rice, S. Ha, R.I. Masel, P. Waszczuk, A. Wieckowski, T. Barnard, *J. Power Sources*, 111 (2002) 83-89.
2. H. Meng, C. Wang, P.K. Shen, G. Wu, *Energy Environ. Sci.* , 4 (2011) 1522-1526.
3. S. Ha, B. Adams, R.I. Masel, *J. Power Sources*, 128 (2004) 119-124.
4. I.M. Al-Akraa, A.M. Mohammad, M.S. El-Deab, B.E. El-Anadouli, *Int. J. Electrochem. Sci.* , 7 (2012) 3939-3946.
5. C. Rice, S. Ha, R.I. Masel, A. Wieckowski, *J. Power Sources*, 115 (2003) 229-235.
6. H. Meng, S. Sun, J.-P. Masse, J.-P. Dodelet, *Chem. Mater.* , 20 (2008) 6998-7002.
7. V. Mazumder, S. Sun, *J. Am. Chem. Soc*., 131 (2009) 4588-4589.
8. Z. Cui, P.J. Kulesza, C.M. Li, W. Xing, S.P. Jiang, *Int. J. Hydrogen Energy*, 36 (2011) 8508-8517.
9. Y.Z. Fu, Y. Yang, *Int. J. Electrochem. Sci.* , 7 (2012) 106-119.
10. F. Godinez-Salomon, E. Arce-Estrada, M. Hallen-Lopez, *Int. J. Electrochem. Sci.* , 7 (2012) 2566-2576.
11. Z. Bai, L. Yang, L. Li, J. Lv, K. Wang, J. Zhang, *J. Phys. Chem*. C, 113 (2009) 10568-10573.
12. X. Chen, G. Wu, J. Chen, X. Chen, Z. Xie, X. Wang, *J. Am. Chem. Soc*., 133 (2011) 3693-3695.

13. S. Zhang, Y. Shao, H.-g. Liao, J. Liu, I.A. Aksay, G. Yin, Y. Lin, *Chem. Mater.* , 23 (2011) 1079-1081.
14. M. Hakamada, M. Mabuchi, *MATERIALS TRANSACTIONS*, 50 (2009) 431-435.
15. C. Jung, C.M. Sánchez-Sánchez, C.-L. Lin, J.n. Rodríguez-López, A.J. Bard, *Anal. Chem*., 81 (2009) 7003-7008.
16. C. Xu, Y. Liu, J. Wang, H. Geng, H. Qiu, *J. Power Sources*, 199 (2012) 124-131.
17. L. Chen, H. Guo, T. Fujita, A. Hirata, W. Zhang, A. Inoue, M. Chen, *Adv. Funct. Mater*. , 21 (2011) 4364-4370.
18. R. Wang, S. Liao, S. Ji, *J. Power Sources*, 180 (2008) 205-208.
19. C. Du, M. Chen, W. Wang, G. Yin, *ACS Appl. Mater. Interfaces* 3(2010) 105-109.
20. C. Du, M. Chen, W. Wang, G. Yin, P. Shi, *Electrochem. Commun*., 12 (2010) 843-846.
21. Y. Gao, G. Wang, B. Wu, C. Deng, Y. Gao, *J. Appl. Electrochem*., 41 (2011) 1-6.
22. B.M. Leonard, Q. Zhou, D. Wu, F.J. DiSalvo, *Chem. Mater.* , 23 (2011) 1136-1146.
23. R. Li, Z. Wei, T. Huang, A. Yu, *Electrochim. Acta*, 56 (2011) 6860-6865.
24. B. Du, S.A. Rabb, C. Zangmeister, Y. Tong, *PCCP* 11 (2009) 8231-8239.
25. Y. Huang, X. Zhou, M. Yin, C. Liu, W. Xing, *Chem. Mater*. , 22 (2010) 5122-5128.
26. W. Zhou, J.Y. Lee, *Electrochem. Commun*., 9 (2007) 1725-1729.
27. H. Wang, V. Linkov, S. Ji, W. Zhang, Z. Lei, R. Wang, *S. Afr. J. Chem*. , 65 (2012) 69-74.
28. H. Wang, S. Ji, W. Wang, V. Linkov, S. Pasupathi, R.F. Wang, *Int. J. Electrochem. Sci*. , 7 (2012) 3390-3398.
29. R. Wang, H. Wang, B. Wei, W. Wang, Z. Lei, *Int. J. Hydrogen Energy*, 35 (2010) 10081-10086.
30. H. Wang, R. Wang, H. Li, Q. Wang, J. Kang, Z. Lei, *Int. J. Hydrogen Energy*, 36 (2011) 839-848.
31. X.L. Wang, H. Wang, R.F. Wang, Q.Z. Wang, Z.Q. Lei, *J. Solid State Electrochem*. , 16 (2012) 1049-1054.
32. X.L. Wang, H. Wang, Z.Q. Lei, Z. Zhang, R.F. Wang, *Chin. J. Catal*. , 32 (2011) 1519-1524.
33. J.L. Haan, K.M. Stafford, R.I. Masel, *J. Phys. Chem*. C, 114 (2010) 11665-11672